Controlled resonant tunneling in a coupled double-quantum-dot system

Gou Shinkai,[a] Toshiaki Hayashi, Yoshiro Hirayama,[b] and Toshimasa Fujisawa[c]
NTT Basic Research Laboratories, NTT Corporation, 3-1 Morinosato-Wakamiya, Atsugi 243-0198, Japan

(Received 11 October 2006; accepted 22 January 2007; published online 9 March 2007)

The authors investigate electrostatic coupling between two double quantum dots (DQDs) defined in an AlGaAs/GaAs heterostructure by measuring the correlation between resonant tunneling currents through the DQDs. Resonant tunneling in one DQD can be controlled by the charge state of the other DQD. This controlled resonant tunneling is consistent with the capacitance model for the geometry and can be used to investigate the statistics of single-electron charge states in the DQD. The observed electrostatic coupling is strong enough to perform two-qubit quantum gates both for charge- and electron-spin-based qubit schemes. © *2007 American Institute of Physics*.
[DOI: 10.1063/1.2709905]

A double quantum dot (DQD) provides a highly tunable quantum system, in which the electrochemical potential of each dot and tunneling coupling between the two dots can be independently adjusted by gate voltages.[1] When one electron occupies the DQD, the ground and the first excited states of the system can be described as a superposition of two charge states delocalized over the two dots (charge qubit). Coherent charge oscillations have been demonstrated by driving the system nonadiabatically with a high-speed voltage pulse.[2] Owing to its large electric dipole, single-shot measurement and dipolar interaction between neighboring qubits are expected.[3,4] On the other hand, when two electrons occupy the DQD (one in each dot), one can use the spin singlet and one of the triplet states having the zero z component as qubit bases (ST_0 spin qubit).[5] Since tunneling between the two dots is allowed only for the singlet (otherwise Pauli spin blockade), the ST_0 spin qubit has a finite electric dipole that can be used to interact with neighboring qubits.[6,7] A DQD with more than two electrons can be considered as effectively a one—or two-electron system by neglecting electron pairs in the inner shells, unless high-spin states appear. For those integrated-qubit systems, strong dipole coupling is essential for realizing controlled quantum operations. In order to investigate the realistic parameters for the dipolar coupling, we fabricated two sets of DQDs connected to source and drain electrodes, which are electrostatically coupled to each other but isolated for conduction. The observed resonant tunneling current through each DQD is influenced by the charge state of the other DQD, which is consistent with the capacitance model. The estimated dipolar coupling is sufficiently large to perform controlled two-qubit operation, considering realistic tunneling coupling obtained in similar devices.

Figure 1(a) shows a scanning electron micrograph of a control sample fabricated in a standard GaAs/AlGaAs heterostructure (two-dimensional electron gas located 90 nm below the surface). By applying appropriate voltages to the gates (labeled as G's), two DQDs composed of four dots (d_{1L} and d_{1R} for DQD1 and d_{2L} and d_{2R} for DQD2) are formed between the sources (S_1 and S_2) and drains (D_1 and D_2). Each quantum dot contains about ten electrons, but we consider an *excess* electron in each DQD in the following discussions. No bias polarity dependence is seen in the measurement, from which we assume effective one-electron DQDs, as in Ref. 2. All measurements were carried out in a dilution refrigerator at about 50 mK at zero magnetic field. In order to ensure independent current measurement for the two DQDs, the voltage on the isolation gate G_{iso} was adjusted so that the leakage current between the channels would be much less than 1 fA. A large negative voltage on G_{iso}, that is, too large, however, decreases the Coulomb interaction of interest. This adjustment was important in the following observation. Since we wanted to investigate the electrostatic coupling in this work, we adjusted the two DQDs in the weak coupling regime, where sharp resonant tunneling peaks are strongly influenced by the charge state of

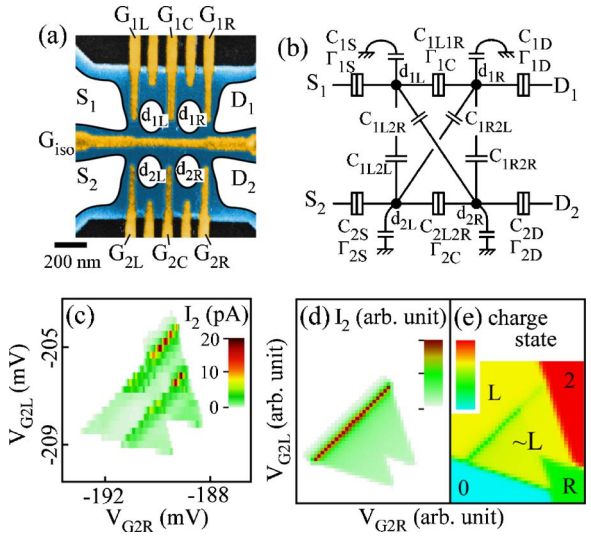

FIG. 1. (Color online) (a) Colored scanning electron micrograph of a control device. Four quantum dots (white circles) are formed by dry etching (upper and lower black regions) and Schottky gates (gold regions). (b) Equivalent circuit model. (c) Current I_2 through DQD2. [(d) and (e)] Calculated I_2 (d) and charge state (e) of DQD2. Plausible parameters were used to simulate (c). The charge states are displayed by considering a virtual charge detector that is more sensitive to the left dot of the DQD and less sensitive to the right dot and shown on a color scale in the order of blue (0), green (R), yellow (L), and red (2) for the corresponding charge states.

[a]Also at: Tokyo Institute of Technology, 2-12-1, O-okayama, Meguro, Tokyo 152-8550, Japan.
[b]Present address: Department of Physics, Tohoku University, Sendai, Miyagi 980-8578, Japan.
[c]Also at: Tokyo Institute of Technology, 2-12-1, O-okayama, Meguro, Tokyo 152-8550, Japan; electronic mail: fujisawa@nttbrl.jp

the other DQD. In this case, single-electron sequential tunneling rather than coherent tunneling describes the transport.

First, we introduce an equivalent circuit model [Fig. 1(b)], where the quantum dots (solid circles), sources, and drains are connected by capacitors and tunneling barriers (characterized by capacitances C's and tunneling rates Γ's). For simplicity in the simulation, we consider the ground state of one-electron charge state in each dot. Thus, the charge state of each DQD takes no electron ("0"), one electron in the left ("L") or right ("R") dot, or two electrons in the DQD ("2"). Corresponding electrochemical potentials μ_{im} for charge state m in the ith DQD can be calculated from the standard capacitance model taking into account the charge states of the other DQD. Tunneling rates at outer barriers (e.g., Γ_{1S} and Γ_{1D} for DQD-1) are well described by energy-independent tunneling probabilities.[1] In contrast, the interdot tunneling rates Γ_{1C} and Γ_{2C} comprise the elastic tunneling rate, which has a sharp peak at the resonant condition (e.g., $\mu_{1L}=\mu_{1R}$ for DQD1), and the relatively small inelastic tunneling rate, which describes the phonon emission process.[8,9] By solving rate equations that involve 16 charge states (n,m), where n and m ($\in\{0,\mathrm{L},\mathrm{R},2\}$) are charge states, respectively, in DQD1 and 2, the occupation probabilities for each charge state and tunneling current through each DQD can be calculated.

Figure 1(c) shows the experimental current I_2 through DQD2 in the V_{G2L}-V_{G2R} (voltages on gates G_{2L} and G_{2R}) plane at a large source-drain bias voltage of $V_2=500\ \mu$V. Typical transport characteristics of a DQD are resolved. The two resonant tunneling peaks are associated with the alignment of the ground state in dot d_{2L} with the ground state (upper peak) or the excited state (lower peak) in dot d_{2R}. Faint inelastic current is observed in the overlapped triangular regions. These behaviors are well reproduced in the simulation if the charge state of the other DQD is unchanged. The current profile and charge state obtained with plausible parameters are shown in Figs. 1(d) and 1(e). The charge state is well defined to one of the four states (0, L, R, and 2) outside the triangles (Coulomb blockade regions). Inside the triangles, the finite current implies that the charge state is randomly distributed with time.[10] However, it is practically dominated by one state (L in this case) if the inelastic tunneling is so weak that the electron gets stuck in the left dot. Therefore, we focus on this weak coupling regime, where the barely measurable inelastic current is much smaller than the sharp elastic current.

To obtain the electrostatic coupling between the two DQDs, we measured the shift of resonant conditions in one DQD when the charge state of the other DQD changed. In practice, as shown in Fig. 2, we swept V_{G1L} and V_{G2L} simultaneously in the same direction (y axis) and V_{G1R} and V_{G2R} simultaneously in the opposite direction (x axis) and simultaneously measured the currents I_1 and I_2, respectively, for DQD1 and 2. In contrast to a single DQD, some traces of resonant peaks split into some pieces (the spacing marked α, β, γ, and δ), and triangular conductive regions shifted at some points (marked a, b, c, and d). We determined the boundary of charge states by extrapolating the triangular conductive regions for each DQD (solid lines). The determined boundaries in each panel are also shown in the other panel by dashed lines. Then, one can notice that the shifts of the features in one DQD coincide with the charge boundaries of the other, indicating Coulomb interaction. Actually, some

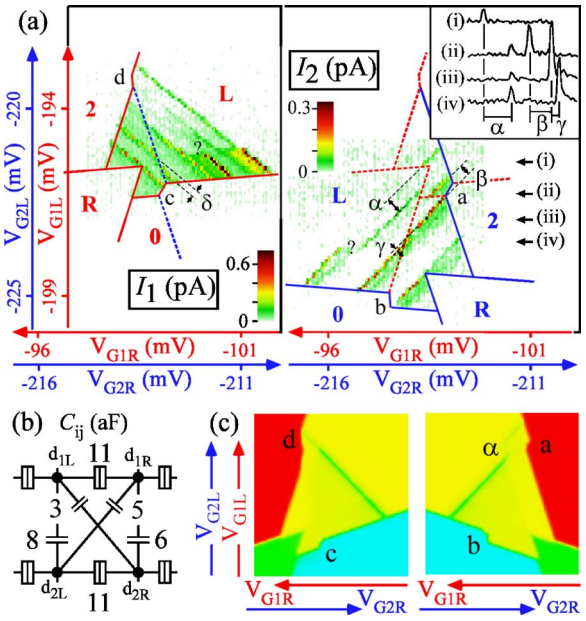

FIG. 2. (Color online) (a) I_1 and I_2 simultaneously obtained with the two-dimensional sweep of combination axes; V_{G2L} and V_{G1L} for the vertical (y) axis and V_{G2R} and V_{G1R} for the horizontal (x) axis. The solid lines represent charge boundaries of each DQD and the dashed lines are those of the other DQD. Some shifts of resonant peaks and charge boundaries are labeled. The inset of the right panel shows the current profiles at some V_{G2L} and V_{G1L} conditions (i)–(iv). Each profile is offset horizontally to show up the shifts α, β, and γ. (b) Coupling capacitances in the coupled DQDs. (c) Charge states of DQD1 (left panel) and DQD2 (right panel) calculated with the capacitances in (b). Color scale is same as in Fig. 1(e).

unknown shifts of resonant peaks were observed in the experiment (marked ?), which might have arisen from background charge trapping in the device. The shifts that occurred in both DQDs originate from interaction between the two DQDs.

In the capacitance model of Fig. 1(b), the shift is characterized by the energy shift U_{ij} of the electrostatic potential of dot i with respect to charging dot j, which is expressed analytically as $U_{ij}=U_{ji}=eC_{ij}/C_{\Sigma i}C_{\Sigma j}$ approximated for the small coupling limit $C_{ij}\ll C_{\Sigma i}$, $C_{\Sigma j}$. Here, $C_{\Sigma i}$ is the total capacitance seen from dot i and C_{ij} is the coupling capacitance. For instance, the spacing of the resonant tunneling peak at β corresponds to $U_{2L1L}-U_{2R1L}$, which is the difference in the electrostatic potential between d_{2L} and d_{2R} induced by charging d_{1L} (DQD1 is changed from 0 to L). Data in Fig. 2 indicate that $U_{2L1L}-U_{2R1L}=60\ \mu$eV. Similarly, we obtained $U_{2R1R}-U_{2L1R}=10\ \mu$eV for γ and $U_{2L1L}+U_{2R1R}-U_{2R1L}-U_{2L1R}=70\ \mu$eV for α. These values are consistent with each other. In this way, we obtained $U_{1L2L}=100\ \mu$eV, $U_{1R2R}=70\ \mu$eV, $U_{1R2L}=60\ \mu$eV, $U_{1L2R}=40\ \mu$eV, and corresponding capacitances as shown in Fig. 2(b). Figure 2(c) shows the calculated average charge state of DQD1 and 2 with the obtained capacitances, which clearly reproduces the shift of charge boundaries (marked a, b, c, and d) and the resonant condition (α). Therefore, the capacitance model well describes all of the shifts. It should be noted that the shift of the resonant peaks is much greater than their width (about 5 μeV), as shown in the current profile [inset of the right panel in Fig. 2(a)]. The well-separated peak structure allows us to investigate the statistics of charge states in a DQD even when time-resolved measurement is not available. Here, we shall determine all tunneling rates in DQD1

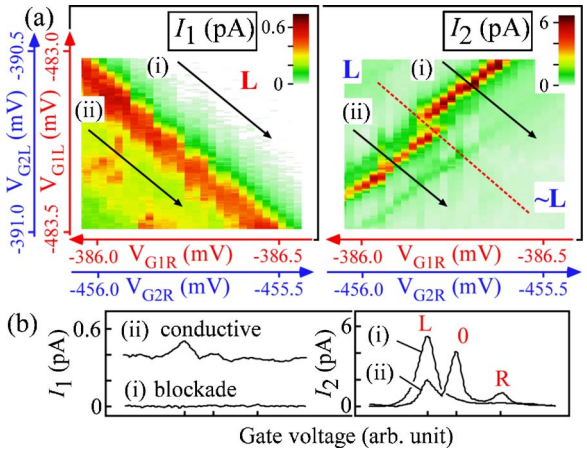

FIG. 3. (Color online) (a) I_1 and I_2 simultaneously obtained with the two-dimensional sweep of V_{G2L} and V_{G1L} for the vertical (y) axis and V_{G2R} and V_{G1R} for the horizontal (x) axis. (b) I_1 and I_2 traces along lines (i) and (ii) in (a). The gate voltages are different from that in Fig. 2, since the data set was measured after a thermal cycle up to room temperature.

by measuring the current spectrum of DQD2. For this purpose, inelastic current through DQD1 was made comparable to the elastic current by adjusting the gate voltage on G_{1C}, while DQD2 was kept in the weak coupling regime. Figure 3(a) shows current profiles I_1 and I_2 in the combined gate voltage plain (V_{G1L}, V_{G2L})-(V_{G1R}, V_{G2R}). We focus on a small region, where resonant tunneling peaks for DQD1 and 2, seen as a diagonal trace in each panel and cross at the center of the traces. The charge state of the DQD1 is well defined as L in the upper-right half of the (left) panel, while it should largely fluctuate in the lower-left conductive region. Distribution of the charge fluctuation is seen in current profile I_2 in the right panel, where the single peak in the upper-left region is splited into three peaks in the lower-left region. For clarity, current along diagonal lines (i) and (ii) is plotted in Fig. 3(b), where energy offset $\mu_{1L}-\mu_{1R}$ of DQD1 is maintained constant for each trace. The peak in I_2 appears at different conditions when DQD1 takes the charge states L, R, and 0. The relative peak height reflects the average dwell time for corresponding charge states, from which we approximately obtained $\Gamma_{1L} \sim 7$ MHz, $\Gamma_{1C} \sim 3$ MHz, and $\Gamma_{1L} \sim 1.5$ MHz, assuming that these tunneling rates are unaffected by the charge state. Basically, we can determine all parameters in the model circuit of Fig. 1(b). Moreover, one can see that I_1 is also affected by the charge state of DQD2 [small peaks in the left panel of Fig. 3(b)], which actually must be taken into account in estimating the precise value of Γ's.

Coulomb interaction between two isolated electrical channels has been discussed in many devices. For example, current through a semiconductor point contact is influenced (typically 5%) by charging single or double quantum dot in a neighboring channel.[10,11] Cross correlation noise measurement of tunneling currents through isolated quantum dots has revealed the presence of Coulomb interaction between the dots fabricated in close proximity.[12] However, the interaction in these semiconductor devices remains in a weak modulation of current. An additional floating gate between the dots is proposed to enhance the interaction. Our observation indicates that the single-electron charge state in one DQD can control the resonant tunneling of the other DQD. This controlled resonant tunneling is desirable for correlating two tunneling currents as well as for correlating two qubits. We believe that fine adjustment of isolation gate G_{iso} is required but sufficient for the controlled resonant tunneling.

Finally, we discuss the feasibility of two-qubit operation in the charge qubit scheme. Charge states L and R having an electric dipole constitute the charge qubit bases. The relevant dipole coupling energy is $\Delta = U_{2L1L} + U_{2R1R} - U_{2R1L} - U_{2L1R} = 70$ μeV, which is observed as spacing α in Fig. 2(a). The Hamiltonian of the two-qubit system can be written as $H = \Sigma_{i=1}^{2}((\varepsilon_i/2)\sigma_{iz} + T_{Ci}\sigma_{ix}) + (\Delta/2)\sigma_{1z}\sigma_{2z}$, where σ_{ix} and σ_{iz} are the Pauli matrices for the ith qubit bases. Here, $\varepsilon_i = \mu_{iL} - \mu_{iR}$ and T_{Ci} are the energy offset and tunneling coupling energy, respectively. We assume realistic parameters for coherent tunneling inside the DQDs ($T_{C1} = T_{C2} = 10$ μeV obtained in a similar device in Ref. 2) and neglect coupling to the source and drain contacts for simplicity. Two-qubit operation can be performed with proper ε_1 and ε_2. For instance, controlled-rotation operation for the target qubit ($i=2$) may be approximately performed at $\varepsilon_1 = 0$ and $\varepsilon_2 = \Delta$, where the coherent resonant tunneling of the target qubit is expected only for the logical one state in the control qubit ($i=1$) (controlled resonant tunneling). Since Δ is much greater than T_{Ci}, the gate fidelity at the approximated condition can be sufficiently high (more than 95% in our simulation). Therefore, two-qubit operation may be feasible in semiconductor quantum dots. A similar argument can be made for spin-based qubits.

In summary, Coulomb interaction in a coupled DQD system was studied by resonant tunneling characteristics and interpreted by a capacitance model. The observed interaction is strong enough to induce controlled resonant tunneling and encourages experiments for two-electron correlation in semiconductor quantum dots.

This work was supported by the Strategic Information and Communications R&D Promotion Program (SCOPE) from the Ministry of Internal Affairs and Communications of Japan and by a grant-in-aid for scientific research from the Japan Society for the Promotion of Science.

[1] W. G. van der Wiel, S. De Franceschi, J. M. Elzerman, T. Fujisawa, S. Tarucha, and L. P. Kouwenhoven, Rev. Mod. Phys. **75**, 1 (2003).
[2] T. Hayashi, T. Fujisawa, H. D. Cheong, and Y. Hirayama, Phys. Rev. Lett. **91**, 226804 (2003).
[3] A. Barenco, D. Deutsch, A. Ekert, and R. Jozsa, Phys. Rev. Lett. **74**, 4083 (1995).
[4] L. Fedichkin, M. Yanchenko, and K. A. Valiev, Nanotechnology **11**, 387 (2000).
[5] J. R. Petta, A. C. Johnson, J. M. Taylor, E. A. Laird, A. Yacoby, M. D. Lukin, C. M. Marcus, M. P. Hanson, and A. C. Gossard, Science **309**, 2180 (2005).
[6] J. M. Taylor, H.-A. Engel, W. Dür, A. Yacoby, C. M. Marcus, P. Zoller, and D. Lukin, Nat. Phys. **1**, 177 (2005).
[7] R. Hanson and G. Burkard, Phys. Rev. Lett. **98**, 056801 (2007).
[8] T. Fujisawa, T. H. Oosterkamp, W. G. van der Wiel, B. W. Broer, R. Aguado, S. Tarucha, and L. P. Kouwenhoven, Science **282**, 932 (1998).
[9] T. Brandes and B. Kramer, Phys. Rev. Lett. **83**, 3021 (1999).
[10] T. Fujisawa, R. Tomita, T. Hayashi, and Y. Hirayama, Science **312**, 1634 (2006).
[11] M. Field, C. G. Smith, M. Pepper, D. A. Ritchie, J. E. F. Frost, G. A. C. Jones, and D. G. Hasko, Phys. Rev. Lett. **70**, 1311 (1993).
[12] D. T. McClure, L. DiCarlo, Y. Zhang, H.-A. Engel, C. M. Marcus, M. P. Hanson, and A. C. Gossard, Phys. Rev. Lett. **98**, 050502 (2007).